Interphase Modeling of Copper-Epoxy Particulate Composites Subjected to Static and Dynamic Loading

G. C. Papanicolaou,[1] A. G. Xepapadaki,[1] A. Kotrotsos,[1] D. E. Mouzakis[2]

[1]*Composite Materials Group, Department of Mechanical and Aeronautical Engineering, University of Patras, Patras 26500, Greece*
[2]*Department of Materials Science, University of Patras, Patras 26500, Greece*

Received 27 November 2007; accepted 18 January 2008
DOI 10.1002/app.28152
Published online 15 April 2008 in Wiley InterScience (www.interscience.wiley.com).

ABSTRACT: In this investigation, the static and dynamic behavior of copper-filled epoxy particulate composites has been experimentally studied. The influence of particle-weight fraction (0–25%), on the static behavior and filler concentration, temperature and frequency on the dynamic behavior of the mentioned particulate composites was thoroughly studied. Experimental results for the static three-point bending modulus were compared with respective theoretical predictions derived from that existing in literature semiempirical models. Results were also compared with predictions derived by the application of the interphase model previously developed by the first author for the evaluation of the elastic modulus in particulate composites, taking into account the effect of filler-matrix adhesion. It was found that the predicted values as derived from the application of the interphase model were in better agreement with experimental findings when compared with respective predictions derived from other models. Polymer-filler degree of adhesion was also studied by applying the Turcsànyi model. Extended SEM investigations and DMA tests were also made to support both experimental and theoretical findings. © 2008 Wiley Periodicals, Inc. J Appl Polym Sci 109: 1150–1160, 2008

Key words: composites; electron microscopy; glass transition; interfaces; modeling

INTRODUCTION

Polymers are under investigation for many years and constitute a significant research area in materials science and technology. To improve their stiffness, tensile strength, and fracture toughness, polymers are filled with inorganic particles. Polymer composites show attributes, which are combination of their components properties. Polymeric particulate composites are widely used in engineering applications not only because of their desirable thermomechanical properties but also due to relatively low manufacturing cost. The macroscopic isotropy of these composites is also quite attractive for mechanical design.

Damage evolution depends on the interface between matrix and reinforcements, the chemical structure, and the crosslink density, when thermoset resins and metallic fillers are combined, the shape of the filler, the aspect geometry, and the filler-volume fraction. First of all, Griffith[1] investigated the energy-absorbing process, which was the production of surface energy and increase of total relative fracture surface increases toughness. Brown[2] examined and proved that the toughness is due to debonded particles acting as voids and causing more local energy absorbing processes. Agari and Uno[3] have worked on thermal and electrical conductivities of polyethylene filled with copper particles and polymethyl methacrylate filled with aluminum particles. Kerkhof[4] studied the variation of crack-front shape in a systematic way and for these reasons, he has used ultrasonic fractography. A great work on thermal, rheological, and mechanical behavior of aluminum- and nickel-filled polypropylene has been done by Maiti and Mahaparto.[5,6] Leidner and Woodhams[7] examined the dependence of the fracture strength of the composite upon the strength of the particle/matrix bond in particle-filled polyester resins.

Continuous efforts for the investigation of the overall mechanical and thermal behavior and the interrelation between macroscopic behavior and micromechanical characteristics of metal-filled epoxies were made by Papanicolaou and coworkers.[8–25] The dynamic properties of metal-filled epoxy polymers were studied in Ref. 8 and their thermal properties in Ref. 9. The concept of the polymer-filler boundary interphase has been studied in Ref. 10, while indentation studies in aluminum-filled epoxies were made in Ref. 11. Thermal properties and volume fraction of the boundary interphase in metal-filled epoxies were investigated in Ref. 12. The effect of filler-volume fraction on the crack-propagation behavior of particulate

Correspondence to: G. C. Papanicolaou (gpapan@mech.upatras.gr).

Journal of Applied Polymer Science, Vol. 109, 1150–1160 (2008)

composites was experimentally studied in Ref. 13. The effect of filler-volume fraction and strain rate on the tensile properties of iron-epoxy particulate composites was studied in Ref. 14. Structural integrity studies in particulate composites by means of thermal capacity measurements were made in Ref. 15. The effect of moisture absorption on the thermomechanical properties of particulates was studied in Ref. 16, while the interrelation between moisture absorption, mechanical behavior, and extent of the boundary interphase in particulate composites was studied in Ref. 17. The effect of water and temperature on the flexural properties of particulate composites was studied in Ref. 18. A model for the prediction of the elastic-modulus of particulate composites using the concept of the boundary interphase was developed in Ref. 19. The dependence of the impact strength of particulate composites on the temperature and filler-volume fraction was studied in Ref. 20. A theoretical model for the prediction of thermal-expansion behavior of particulate composites has been developed and predictions were successfully compared with respective experimental results in Ref. 21. The influence of the adhesion bond between matrix and filler on the tensile-strength of particulate-filled polymers was both theoretically and experimentally studied in Ref. 22. Water sorption and temperature effects on the dynamic mechanical-behavior of epoxy-matrix particulates were studied in Ref. 23. The effect of low-energy impact on the tensile strength of coated and uncoated glass particulate composites was studied in Ref. 24. Finally, in a recent publication, a stress analysis of particulate-reinforced polymers by means of the concept of hybrid interphase was presented.[25]

From all the aforementioned research works it can be concluded that matrix-filler degree of adhesion determines in a great extent the overall mechanical, thermal, and viscoelastic behavior of polymer matrix composites. This explains the tremendous amount of experimental and theoretical data that existed in literature, expressing the interest of the international scientific community to elucidate the too many structural parameters related either with the failure modes[26–28] and/or with the prediction of the composite stiffness or strength of this class of composites.[29–42]

The addition of copper fibers to a thermoset polymer matrix, given the correct fiber shape and surface treatment, results in a multifunctional composite with increased mechanical, electrical, and thermal properties. Furthermore, besides improving the fracture and impact toughness of a thermoset polymer matrix, short-shaped copper fibers can also significantly improve the shielding effectiveness (SE) in transmission and the electrical conductivity of the composite.[43] The addition of copper to a polymer matrix also improves the composite's thermal conductivity and diffusivity.[44,45]

This work is an effort to study the static bending and dynamic behavior of copper-filled epoxy particulate composites and to correlate experimental results with respective theoretical predictions based on micromechanics. Several semiempirical models/expressions that existed in literature were used and their predictions were compared with respective experimental results and predictions as derived from the application of the so-called interphase model, which was previously developed by the first of the authors.[19] In addition, the influence of particle-weight fraction (0–25%) on the mechanical and dynamic behavior of these composites was examined.

PREDICTIVE MODELS

Predictive models for the elastic modulus

The mechanical properties of particulate-filled composites are affected by a great number of geometrical, topological, mechanical parameters. Numerous studies have been focused on the micromechanics of particulate-filled composites.[29–42] Unfortunately, the discrepancies between theoretical predictions and experimental data continue to limit the understanding of these composite materials. In all the existing theories, difficulty has been encountered in separating variables such as interfacial adhesion, particle agglomeration, dispersion, and particle shape, all of which affect mechanical behavior. Other parameters such as polymerization-induced stresses and shear effects around filler particles further complicate the prediction.[8–25]

The oldest existing theory refers to inclusions in a viscous matrix and was developed by Einstein.[29] He considered rigid spherical nonsolvated particles in a Newtonian viscous fluid, and his final expression for the prediction of the effective modulus of the particulate composite is as follows:

$$\frac{E_c}{E_m} = 1 + 2.5V_f, \tag{1}$$

where E_c and E_m are the elastic moduli for the composite and the matrix, respectively, and V_f, the filler-volume fraction.

An extension of Einstein's equation is that developed by Guth and Smallwood.[30,31]

$$\frac{E_c}{E_m} = 1 + 2.5V_f + 14.1V_f^2. \tag{2}$$

Next, an equation based on a mathematical theory and valid for polymer-particulate composites when in glassy state was given by Kerner.[32] The final expression of this theory as applied to rigid fillers is as follows:

$$\frac{E_c}{E_m} = 1 + \frac{V_f}{V_m}\left[\frac{15(1-\nu_m)}{8-10\nu_m}\right], \tag{3}$$

where ν_m is the matrix Poisson's ratio and V_m is the matrix volume fraction.

Lewis and Nielsen[33] suggested the following equation for polymer-particulate composites:

$$\frac{E_c}{E_m} = \frac{1+ABV_f}{1-B\psi V_f}, \tag{4}$$

where A is a constant which considers factors such as particle geometry and matrix Poisson's ratio, ν_m, and is given by,

$$A = \frac{7-5\nu_m}{8-10\nu_m}, \tag{5}$$

and B is a constant which depends on the flexural modulus ratio of the filler particles, E_f, and the matrix material, E_m, and is given by,

$$B = \frac{\left(E_f \Big/ E_m\right) - 1}{\left(E_f \Big/ E_m\right) + A}. \tag{6}$$

Finally, if V_f is the filler concentration then ΨV_f is given by the following equation:

$$\psi V_f = 1 - \exp\left(\frac{-V_f}{1-\left(\frac{V_f}{\varphi_m}\right)}\right), \tag{7}$$

where φ_m is the maximum packing fraction which is equal to 0.637 for spherical particles.

The effect of filler agglomeration is taken into account in the following equation proposed by Mooney.[34]

$$\frac{E_c}{E_m} = \exp\left(\frac{2.5V_f}{1-sV_f}\right), \tag{8}$$

where s is a ''crowding factor'' taking values in the range 1–2 depending on the type of particle distribution into the polymer matrix. For closely packed spheres of uniform size, $s = 1.35$.

In the equation proposed by Eilers and Van Dyck,[35]

$$\frac{E_c}{E_m} = \left(1 + \frac{kV_f}{1-S'V_f}\right)^2, \tag{9}$$

where, k and S' are constants usually equal to 1.25 and 1.20, respectively.

Phillips[36] suggested the following expression for the Young modulus of particulate composites assuming a simple model based on a cubic array of equivalent volume fraction to spherical particles dispersed in a continuous phase:

$$\frac{E_c}{E_m} = \frac{X^2}{1-X(1-E_m/E_f)} + (1-X^2), \tag{10}$$

X can be related to the volume fraction of the discontinuous phase, V_f, by an expression of the form,

$$X = (PV_f)^{1/3}, \tag{11}$$

where P is a disposable parameter described as the ''relative volume fraction,'' since it is the ratio of (volume of equivalent cubic particles)/(volume of spherical particles). Phillips has shown that $P = 1$ for cubic particles, and that for spherical particles P is $6/\pi = 1.91$ and $2/\sqrt{3}\pi = 0.37$ for the upper and the lower bound, respectively.

The interphase model

During the manufacturing of particle-reinforced polymers (PRPs), interphases are developed by lying at the close vicinity of the surface of reinforcing fillers. In common PRPs, these intermediate material phases have complex structure, contain voids, microcracks, and several impurities, while matrix macromolecules belonging to these areas are characterized by a reduced mobility, Figure 1. The interphase separating the distinct filler and matrix phases is a region in which filler and matrix are mechanically and chemically combined or indistinct. It may be a diffusion zone or a chemical reaction zone and thus may be studied within the context of a composite material system that acts as a single entity. This system exists when two or more distinct materials interact synergistically to produce a superior material.

A theoretical model for the prediction of the elastic modulus and the Poisson's ratio of polymer matrix particulates, which considers the existence of a particle-matrix inhomogeneous interphase, has been developed by Papanicolaou and coworkers.[20,21] According to this model, the interphase thickness Δr_i and the interphase volume fraction, V_i, is first calculated as follows:

$$\left(\frac{r_f + \Delta r_i}{r_f}\right)^3 - 1 = \frac{\lambda V_f}{1-V_f}, \qquad V_i = \frac{3\Delta r_i V_f}{r_f} \tag{12}$$

where the parameter λ is given by:

$$\lambda = 1 - \frac{\Delta C_p^f}{\Delta C_p^0}, \qquad r_i = r_f + \Delta r_i \tag{13}$$

In which ΔC_p^f and ΔC_p^0 correspond to the abrupt jump in heat capacity observed at the transition

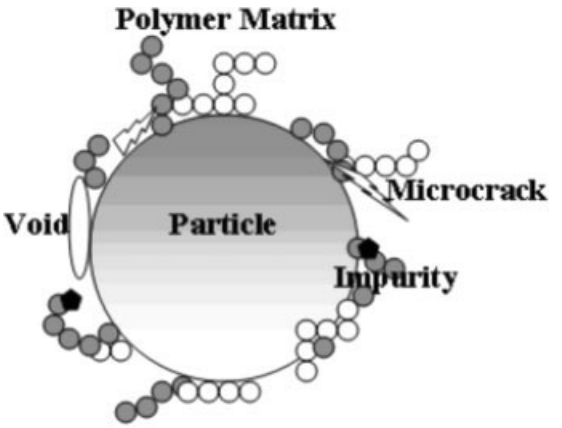

Figure 1 Structural characteristics of the filler-matrix interphase region.

region for the filled and the unfilled polymer, respectively.

Then the interphase Poisson's ratio and the composite Poisson's ratio can be calculated as follows:

$$\nu_i(r) = \frac{\nu_f - \nu_m}{(r_i - r_f)^2} r^2 + \frac{2(\nu_m - \nu_f) r_i}{(r_i - r_f)^2} r + \frac{\nu_f {r_i}^2 + \nu_m {r_f}^2 - 2\nu_m r_f r_i}{(r_i - r_f)^2}, \quad (14)$$

$$\nu_c = \nu_f V_f + \nu_m V_m + \nu_i V_i, \quad (15)$$

Last equation can be written as follows:

$$\nu_c = \nu_f V_f + \nu_m V_m + \frac{3V_f}{{r_m}^3} \int_{r_f}^{r_i} \nu_i r^2 dr. \quad (16)$$

Finally, the modulus of the composite, E_c, can be calculated by the following relation:

$$\frac{(1-2\nu_c)}{E_c} = \frac{(1+\nu_f)^2(1-2\nu_m)^2}{(1-2\nu_f)(1+\nu_m)^2} V_f + \frac{(1-2\nu_m)}{E_m} V_m + \frac{3(1-2\nu_m)^2 V_f}{(1+2\nu_m) r_f^3} \int_{r_f}^{r_i} \frac{(1+\nu_i)^2}{(1-2\nu_i) E_i} r^2 dr. \quad (17)$$

Predictive models for the mechanical strength

In the case of a brittle thermoset polymer, such as epoxy or thermoset polyester, that has relatively low fracture energy, the addition of fillers tends to increase the fracture toughness and the maximum strength at low filler volume fractions. However, above a critical volume fraction, both the fracture energy and the maximum strength decrease. The critical volume fraction at which the maximum fracture energy and/or the maximum strength are attained depends on the filler particle size as well as the interfacial bond between the fillers and the polymer matrix. The larger the particle size, the greater is the critical volume fraction as well as the maximum fracture energy; although the effect of the latter is somewhat conflicting. The maximum strength of a filled polymer is more difficult to predict than the modulus. Unless there is a good bonding between the fillers and the polymer, the fillers do not share much load with the polymer; instead, they merely act as sources of stress concentration. In the case of no adhesion, the mechanical strength of the filled polymer decreases with increasing filler volume fraction.

There have also been some equations reported for estimating the tensile strength of particulate composites. Two of the most common equations concerning the composition dependence of mechanical properties of composites are based on the first power and two-thirds power laws.[37]

$$\sigma_c = \sigma_m(1 + V_f), \quad (18)$$

$$\sigma_c = \sigma_m(1 + V_f^{2/3}). \quad (19)$$

In the two-thirds power law, Nielsen[38]has suggested the use of a parameter S. The maximum value of parameter S is unity for perfect adhesion and lower for poorer adhesion.

$$\sigma_c = \sigma_m(1 + V_f^{2/3})S. \quad (20)$$

Nicolais and Narkis[39] suggested the use of the weightage factor equal to 1.21 as follows:

$$\sigma_c = \sigma_m(1 + 1.21V_f^{2/3}). \quad (21)$$

Gupta and Purwar[40] suggested the addition of S' which reflects the concentration of stresses as follows:

$$\sigma_c = \sigma_m(1 + V_f)S'. \quad (22)$$

Finally, another equation has been suggested by Piggot and Leidner[41] as follows:

$$\sigma_c = \sigma_m(a + bV_f), \quad (23)$$

where the two parameters a and b depend on the size, shape, particles and matrix flexural moduli, and maximum strength.

MATERIALS

Copper fillers (Fig. 2) used in this investigation are spherical in shape having a rather uniform granul-

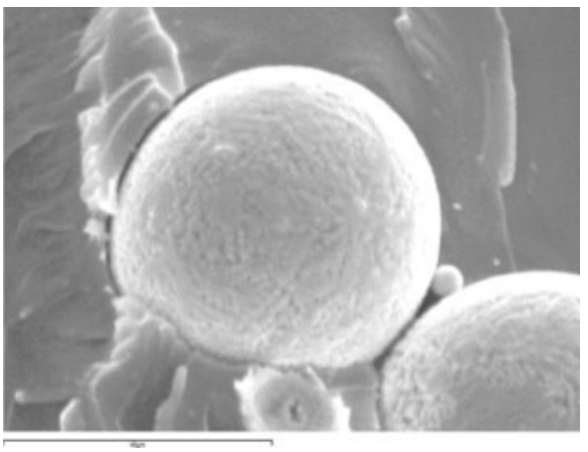

Figure 2 SEM photomicrograph of a copper particle.

ometry with a mean diameter of 40 μm. Polymer composite formulations were prepared by mixing copper particles with an epoxy resin. The epoxy resin used as matrix was derived from a system based on diglycidyl ether of bisphenol A resin (DGEBA, Epikote 828, Shell, Amsterdam, the Netherlands) as prepolymer, with an epoxy equivalent of 185–192, a molecular weight between 370 and 384, and a viscosity of 15,000 mPa/s at 25°C. As curing agent, diethylenetriamine (DETA) was used, that is, a highly reactive amine capable of curing diglycidyl ethers at room temperature. All components of the system were commercial products and were used without purification.

The basic properties of the two main components of the composite material tested are listed in Table I.

SPECIMENS PREPARATION

Copper particles and resin were carefully mixed for 30–40 min, to achieve uniform distribution of grains in the matrix. Proper amounts of the curing agent were then added. The copper-resin mixture was then placed in a vacuum pump for 3 min to reduce voids in the composite. Subsequently, the mixture was poured in Plexiglas molds (90 mm × 95 mm × 3 mm) of suitable capacity. Next, the filled molds were placed in an oven for the curing phase. The following curing process was applied: temperature was raised at 5°C/h from ambient to 80°C and maintained constant for ~24 h. Plates were then removed from the molds and were subsequently cut to the proper dimensions for three-point bending and dynamic mechanical thermal analyses (DMA) testing.

SEM FRACTOGRAPHY

To explain the behavior of the copper-particulate composites in bending, scanning electron microscopy (SEM) photomicrographs were taken and analyzed. In Figure 3, we can see how plain copper particles tend to agglomerate even if they are not embedded into a polymeric matrix. This tendency makes the fabrication procedure more difficult. From the same figures, we can also see that copper particles have perfectly spherical shape of different diameter.

Figure 4 shows typical scanning electron micrographs of the fracture surfaces for the pure polymeric matrix of tested composites under three-point bending conditions. From these photomicrographs it can be observed that pure matrix specimens show shear bands due to inherent softening of the material. Because of the localized softening mechanism, fine deformation bands are obtained in which the shear is highly localized. Once a small region starts to undergo shear yielding it will continue to do so because it has a lower flow stress than the surrounding relatively undeformed regions.

Figure 5 shows scanning electron micrographs of the fracture surfaces of the composites under investigation for varying filler-weight fractions fractured under three-point bending conditions. From these photomicrographs it can be observed that filler aggregation exists in all cases. As it will be discussed later on in the section concerning maximum strength of the composites under investigation, this observation is very important for the explanation of the effect of aggregates on the maximum strength variation with filler loading.

STATIC FLEXURAL TESTING

Three-point bending tests were carried out according to ASTM D 790-99 by means of a conventional Instron type tester (INSTRON 4301, England), at room temperature. Specimens with a gauge length of 63 mm were tested at a constant strain rate of 1.5 mm/min. The repeatability of results confirms the good manufacturing conditions of the specimens as well as the appropri-

TABLE I
Basic Properties of Constituents

		Units	Copper	DGEBA resin
Lame's constants	λ	N/m^2	10.38×10^{10}	3.34×10^9
	μ			1.30×10^9
Flexural modulus	E	N/m^2	4.8×10^{10}	3.53×10^9 (T = 20°C, t =15 s)
Poisson's ratio	ν	N/m^2	0.34	0.36 (T = 20°C, t = 15 s)
Density	ρ	N/m^2	6.68	1.19

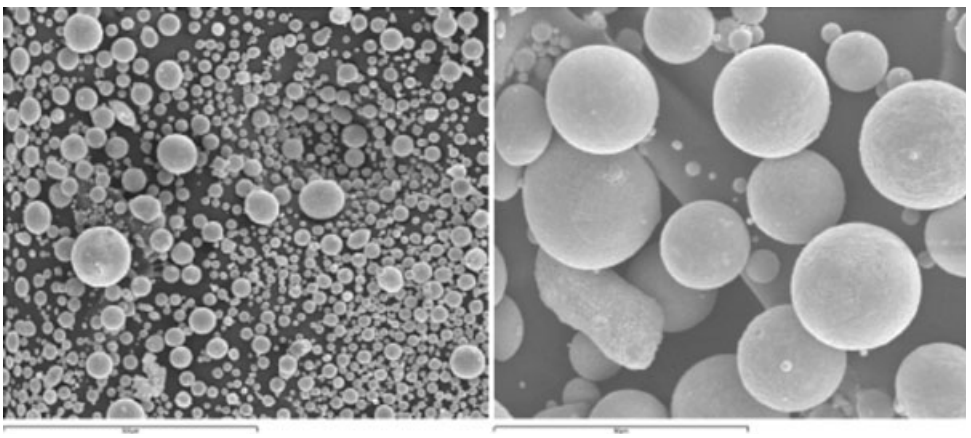

Figure 3 Scanning electron micrographs showing the tendency for agglomeration of copper particles.

ate selection of the curing processing conditions.[10–12] The samples were ~ 90-mm long, 12-mm wide, and 3-mm thick.

DYNAMIC MECHANICAL TESTING

Mechanical spectroscopy is the scientific method to estimate the ability of the materials to store or dissipate energy during their deformation. The material stores energy, when strained and it yields it back, with a rate, which is typical for the specific material. Most of the materials show a divergence from the ideal elastic behavior, so that they loose some of the deformation energy in the form of heat. The properties that are of interest in the mechanical spectroscopy are the resonant frequency and the dissipation factor. DMA is a technique measuring these properties.

Specimens of 60 mm × 12 mm × 3 mm of particulate composites were made and DMA were performed on a DMA Q800 V3.13 Build 74 apparatus (USA) under 5 Hz three-point bending mode and a temperature ramp of 3°C/min. The amplitude of the harmonic loading was 25 μm.

The temperature range was from 25 to 180°C, and the aim is to estimate the variation of the T_g, the dynamic modulus (E'), and the loss factor (tan δ), with temperature for different percentages of particles.

Results are provided in the form of curves, tan δ or E' or E'' versus temperature. T_g was estimated from the temperature where the tan δ curve shows the peak.

RESULTS AND DISCUSSION

Flexural modulus

The stress–strain behavior of the copper-particulate composites with different weight fractions is presented in Figure 6. Each value in Figure 6 is the average of three tests. As we can observe, strength is increasing with filler loading and the modulus as well.

Figure 7 shows the variation of the flexural modulus with filler-weight fraction. A comparison between experimental values and predictions as derived from different theories is shown.

As can be seen, a continuous increase of the modulus with filler-weight fraction is observed. This kind of behavior is reasonable since the ratio of the filler modulus to that of the resin exceeds 14:1. Values derived from the application of eq. (10) were

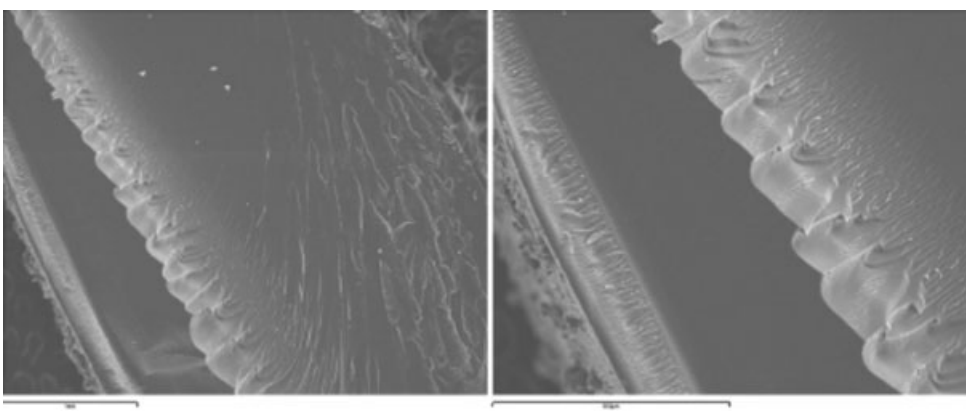

Figure 4 Scanning electron micrographs of fracture surfaces of the pure polymer matrix after three-point bending test.

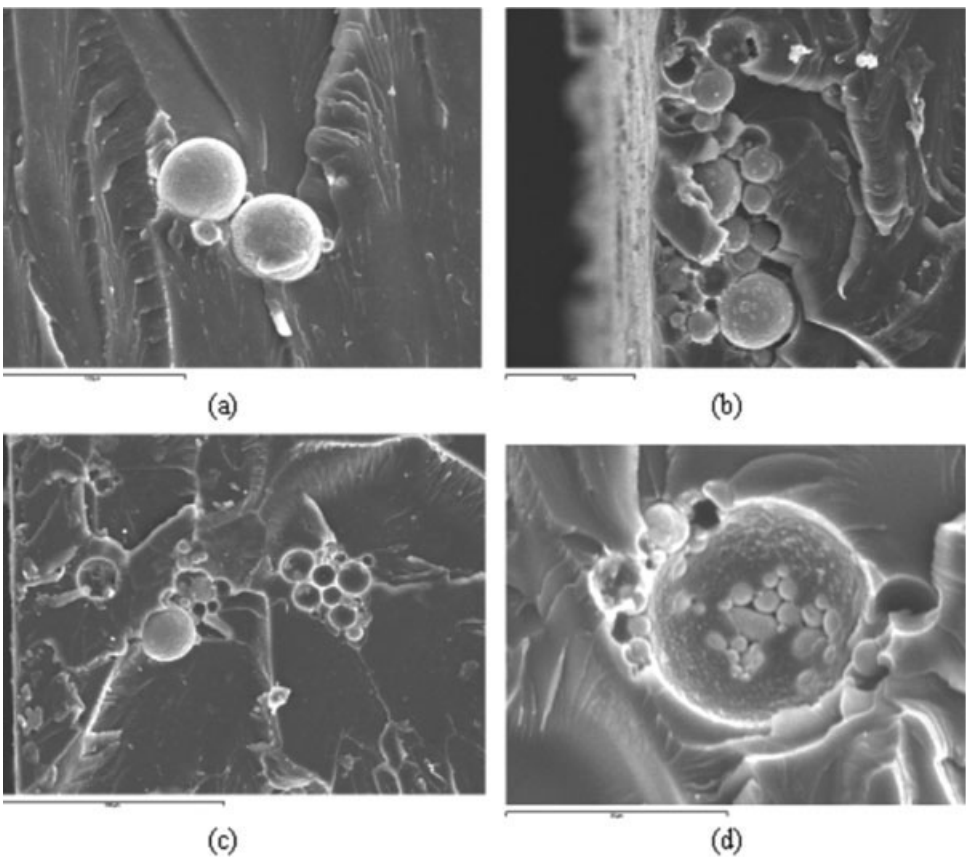

Figure 5 Scanning electron micrographs of fracture surfaces of the copper particle epoxy composites of varying filler weight fraction: (a) 5%, (b) 10%, (c) 15%, and (d) 20%.

obtained for $P = 1.14$, which is the mean value of the upper bound (=1.91) and the lower bound (=0.37). Also, calculated values from eq. (8) were obtained for $s = 1.35$. Calculated values as derived from eq. (9) with $k = 1.25$ and $S' = 1.20$ are also plotted. We can see that values derived from Papanicolaou, Eilers–Van Dyck, and Mooney equations fit quite well with the experimental ones. In contrary

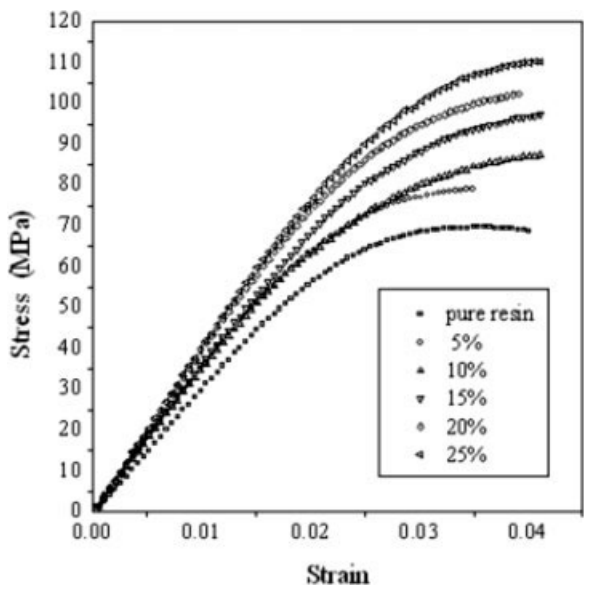

Figure 6 Stress–strain curves for the copper-particulate epoxy composites for various filler-weight fractions.

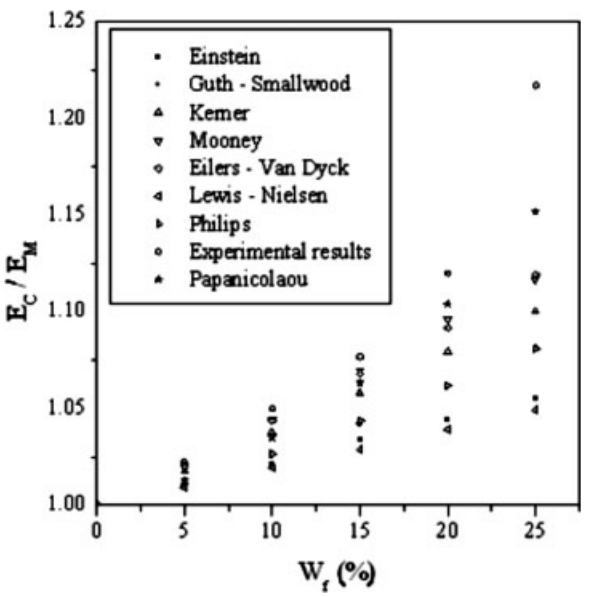

Figure 7 Comparison between experimental values and predictions as derived from several theories for the flexural modulus of the copper particle-epoxy matrix composites investigated.

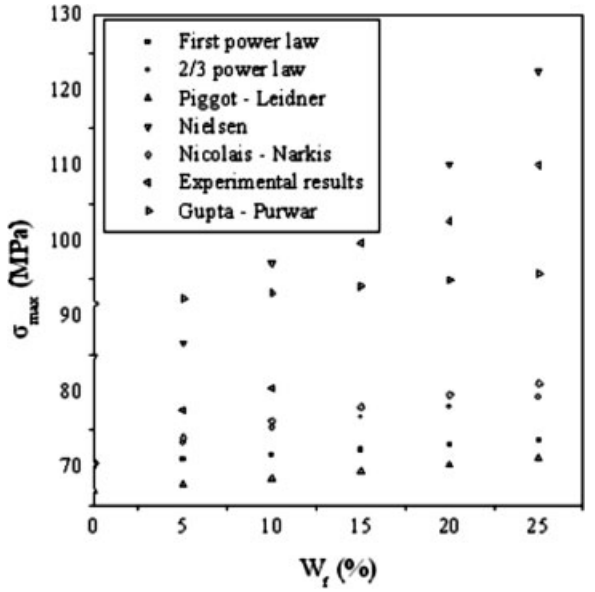

Figure 8 Flexural strength versus filler-weight fraction according to various theories along with respective experimental results.

with all the aforementioned semiempirical models which are applicable under the condition of a curve-fitting procedure, the interphase model which is based on DSC measurements along with a strict mathematical formulation and takes into account the existence of filler-matrix interphase predicts well the experimental results.

Flexural strength

The variation of the flexural strength of the composite under investigation with the filler-weight fraction is shown in Figure 8. In the same figure, respective theoretical predictions have been plotted along with the experimental results. We can see that the flexural strength increases as the weight fraction of copper particles increases. Also, it is clear that there is no theory predicting with accuracy the observed variation of experimentally derived maximum bending strength values. A final observation is that no critical filler-weight fraction is observed. This might be due to the fact that the maximum filler loading of our specimens is 25%, whereas the critical weight fraction can be greater than this value.

The semiempirical equation derived by Turcsànyi et al.[42] is as follows:

$$\sigma_{yc} = \frac{1 - V_f}{1 + AV_f}\,\sigma_{ym}\exp[BV_f], \tag{24}$$

where σ_y is the yield stress and V_f the filler-volume fraction. Symbol c represents the composite and m the matrix. A is a shape parameter and for spherical particles its value is 2.5. B is the parameter involved with the particles-matrix interface properties. If $B = 0$, particles behave like voids. For values $B \leq 3$, the interface is weak.

$$B = \frac{\ln\frac{(1+AV_f)\sigma_{yc}}{(1-V_f)\sigma_{ym}}}{V_f}. \tag{25}$$

From Figure 9, it is observed that B is decreasing with filler-weight fraction.

For $W_f = 5\%$, particle-matrix adhesion is the best, while filler loading increases, adhesion worsens. In any case, from $W_f = 5\%$ up to $W_f = 25\%$, all values of the parameter B are greater than 3, which means that a reinforcing effect is always present.

Dynamic mechanical behavior

Figure 10 depicts the variation of the storage modulus with temperature at fixed frequency ($f = 5$ Hz) and for different filler-weight fractions. For the maximum weight fraction, 25%, storage modulus attains its maximum value, $E' = 4.13$ GPa, whereas for the pure resin, the respective value for E' is only 2.5 GPa.

Figures 11 and 12 show the loss modulus and the tan δ variation with temperature for varying weight fractions, respectively. As one can see, there is no significant change in loss modulus values with filler-weight fraction. According to the results shown in Figure 12, a shift of tan δ peak to higher temperatures with filler-weight fraction is observed.

It is found that when the values of storage modulus E', loss modulus E'', and tan δ are measured for a polymer at a fixed temperature their values

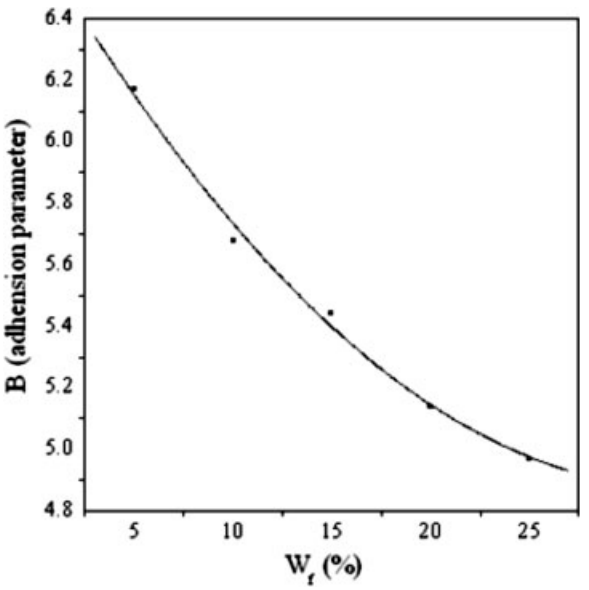

Figure 9 Variation of the adhesion parameter B versus filler-weight fraction.

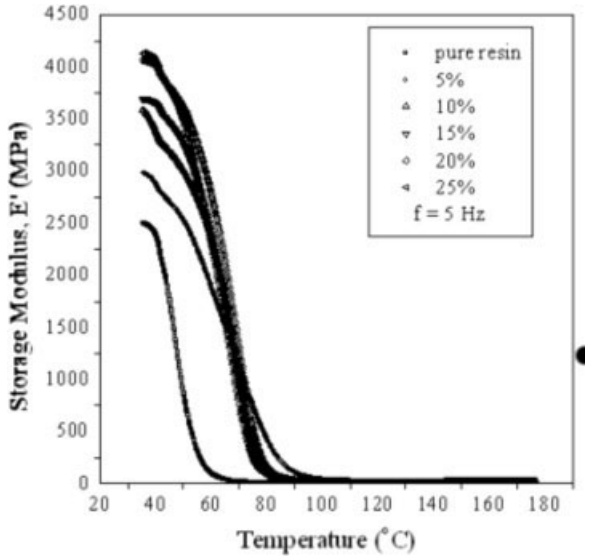

Figure 10 Variation of the storage modulus with temperature for different filler-weight fractions.

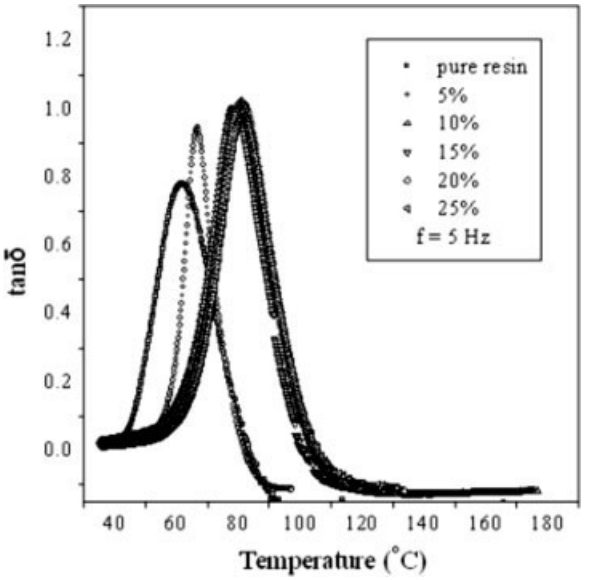

Figure 12 Variation of tan δ with temperature for different filler-weight fraction (0–25%).

depend upon the testing frequency or rate. It is found that tan δ and E'' are usually small at very low and very high frequencies and their values peak at some intermediate frequency. On the other hand, E' is high at high frequencies when the polymer is displaying glassy behavior and low at low frequencies when the polymer is rubbery. The value of E' changes rapidly at intermediate frequencies in the viscoelastic region where the damping is high and E'' and tan δ peak. The frequency dependence of the viscoelastic properties of the materials under investigation as measured at $T = 25°C$ is shown in Figures 13–15. From Figure 13, it can be seen that the maximum value for E' is observed at $W_f = 10\%$, while the minimum is observed for both the pure resin as well at $W_f = 5\%$.

Loss modulus variation with frequency is shown in Figure 14. From this figure it can be seen that loss modulus is maximum for the pure resin and minimum for the maximum weight fraction. Similar observations can be deduced for tan δ variation with frequency as shown in Figure 15.

A comparison between static and dynamic moduli (as measured at $f = 50$ Hz and $T = 25°C$) variation with filler-weight fraction is shown in Figure 16. From this figure it can be concluded as follows: (a)

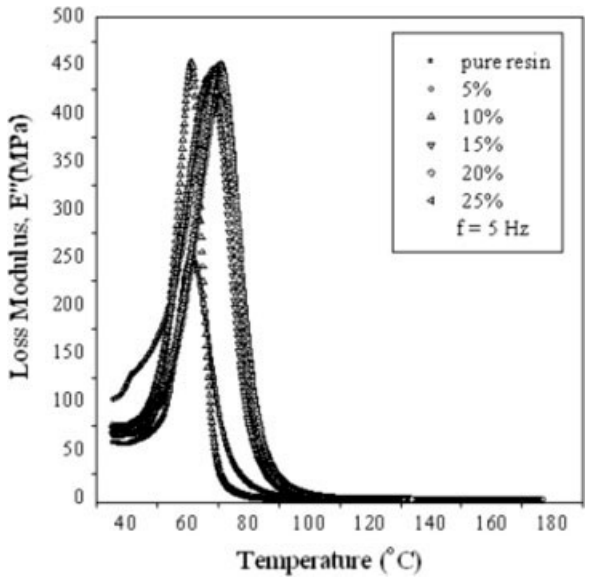

Figure 11 Variation of loss modulus with temperature for different filler-weight fraction (0–25%).

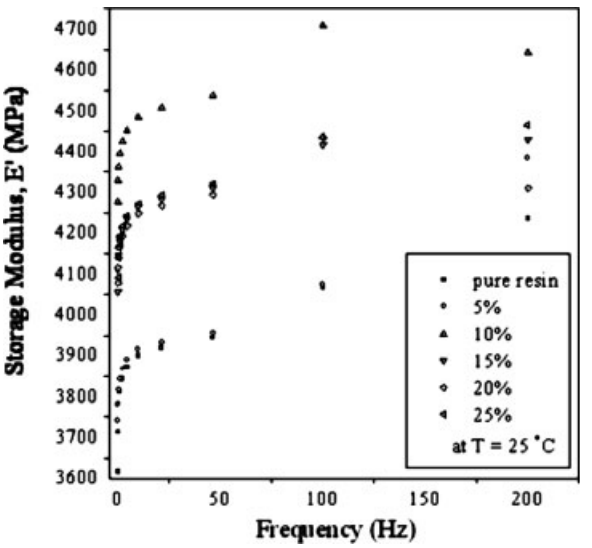

Figure 13 Variation of the storage modulus with frequency (Hz) for different filler-weight fractions.

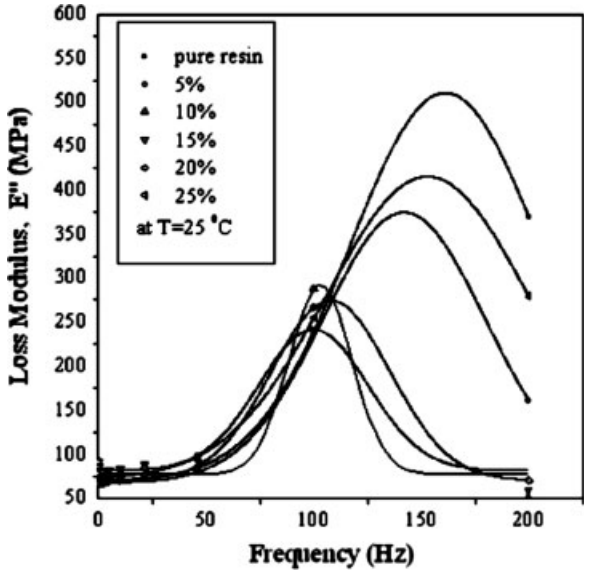

Figure 14 Variation of the loss modulus with frequency for different filler-weight fractions.

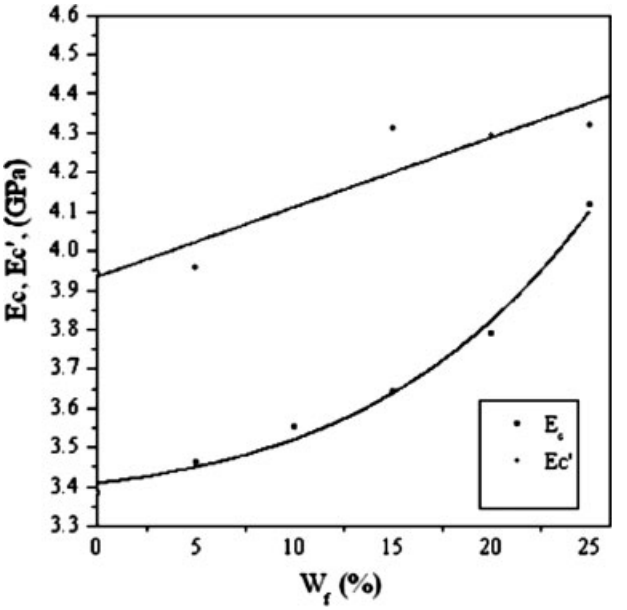

Figure 16 Comparison between static and dynamic modulus (at f = 50 Hz, T = 25°C) for varying filler-weight fraction.

both moduli are increasing functions of filler loading and (b) storage modulus is always higher than the respective value for the bending static modulus.

Finally, Figure 17 shows the variation of the glass transition temperature with filler-weight fraction, which was determined from the peaks of tan δ–temperature curve. From this figure it becomes clear that glass transition temperature is increasing up to W_f = 10% and then it almost remains constant. The increase in T_g appears to be dependent on the filler-weight fraction and is probably due to the immobilization by adsorption of the polymer segments close to the surface of the filler particles. The mechanism by which the adsorption of polymer molecules on the filler surface reduces the number of possible configurations of the polymer molecules is not clear. It may be likened to a mechanical chain with two ends anchored on two filler particles, each polymer coil being depicted as a link in the chain. The mobility of such a mechanical chain is greatly reduced. It should be mentioned that the aforementioned macromolecular constraints exhibit within the polymer-filler interphase area, and that the thickness of which could be significant when compared with the particle size. It seems reasonable to conclude that the polymer mole-

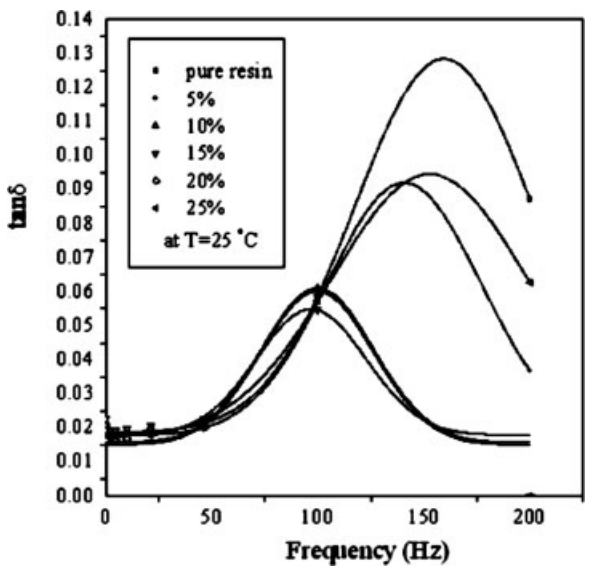

Figure 15 Variation of tan δ with frequency for different filler-weight fractions.

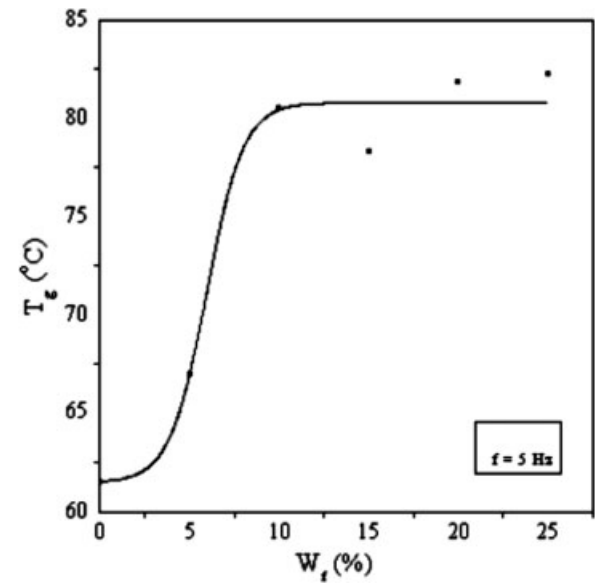

Figure 17 Variation of the glass transition temperature with particle-weight fraction.

cules within the interphase possess properties are different from the unfilled polymer. In addition to this, since any deformation of a polymeric matrix results in nonuniform straining in the vicinity of a filler particle, the localized behavior is nonhomogeneous.

CONCLUSIONS

In this investigation, the static bending and dynamic behavior of copper-filled epoxy particulate composites has been experimentally determined. The influence of particle-weight fraction (0–25%) on both the static and dynamic behavior of the particulate composites is thoroughly studied. A comparison between experimental and theoretical values predicted by several existing in literature models as well as by the interphase model previously developed by the first author for the evaluation of the elastic modulus in particulate composites has been done. From the whole work the following conclusions can be deduced:

As resulted from three-point bending tests, flexural modulus values predicted when applying the interphase model were in better agreement with experimental findings when compared with respective predictions derived from other existed in literature models. At this point it is important to underline that despite the fact that flexural modulus is increasing with filler-weight fraction, the adhesion parameter (B) is decreasing with the increase in copper-filler weight fraction. In all cases, B is always higher than 3 and more specifically, higher than 4.95, which means that reinforcing effects are always present. As for the static flexural strength it was found that a linear increase of the flexural strength with filler-weight fraction up to $W_f = 25\%$ was observed, whereas no theory that exists predicts with accuracy the experimentally observed variation of flexural strength with filler-weight fraction. Finally, according to our experimental findings, no critical filler-weight fraction up to $W_f = 25\%$ was observed.

Next, concerning the dynamic mechanical behavior of copper-epoxy particulates, an increase in storage modulus and a respective decrease in loss modulus and tan δ with filler loading was observed. Finally, a continuous increase of T_g with filler content was found to exist up to $W_f = 10\%$ after which no further variation is observed.

References

1. Griffith, A. A. Phil Trans R Soc A 1921, 221, 163.
2. Brown, S. K. Brit Polym Sci J 1980, 12, 24.
3. Agari, Y., Uno, T. J Appl Polym Sci 1986, 32, 5705.
4. Kerkhof, F. Cement Concr Res 1972, 2, 248.
5. Maiti, S. N.; Mahapatro, P. K. Polym Plast Technol Eng 1991, 30, 559.
6. Maiti, S. N.; Mahapatro, P. K. Polym Compos 1990, 11, 223.
7. Leidner, J.; Woodhams, R. T. J Appl Polym Sci 1974, 18, 1639.
8. Paipetis, S. A.; Papanicolaou, G. C.; Theocaris, P. S. Fiber Sci Technol 1975, 8, 221.
9. Papanicolaou, G. C.; Paipetis, S. A.; Theocaris, P. S. J Appl Polym Sci 1977, 21, 689.
10. Papanicolaou, G. C.; Paipetis, S. A.; Theocaris, P. S. Colloid Polym Sci 1978, 256, 625.
11. Theocaris, P. S.; Paipetis, S. A.; Papanicolaou, G. C. J Appl Polym Sci 1978, 22, 2245.
12. Papanicolaou, G. C.; Theocaris, P. S. Colloid Polym Sci 1979, 257, 239.
13. Theocaris, P. S.; Papanicolaou, G. C.; Papadopoulos, G. A. J Compos Mater 1981, 15, 41.
14. Theocaris, P. S.; Papanicolaou, G. C.; Kontou, E. A. J Reinforced Plast Compos 1982, 1, 206.
15. Theocaris, P. S.; Papanicolaou, G. C.; Sideridis, E. P. J Reinforced Plast Compos 1982, 1, 92.
16. Theocaris, P. S.; Kontou, E. A.; Papanicolaou, G. C. Colloid Polym Sci 1983, 261, 394.
17. Theocaris, P. S.; Papanicolaou, G. C.; Kontou, E. A. J Appl Polym Sci 1983, 28, 3145.
18. Papanicolaou, G. C.; Mercogliano, R. Plast Rubber Process Appl 1986, 6, 229.
19. Sideridis, E. P.; Theocaris, P. S.; Papanicolaou, G. C. Rheol Acta 1986, 25, 350.
20. Papanicolaou, G. C.; Andreopoulos, A. G. Mater Chem Phys 1987, 18, 49.
21. Sideridis, E. P.; Papanicolaou, G. C. Rheol Acta 1988, 27, 608.
22. Papanicolaou, G. C.; Bakos, D. J. J Reinforced Plast Compos 1992, 11, 104.
23. Papanicolaou, G. C.; Pappa, A. J Mater Sci 1992, 27, 3889.
24. Papanicolaou, G. C.; Giannis, S. P.; Imielinska, K. J Mater Sci 2003, 38, 533.
25. Papanicolaou, G. C.; Anifantis, N. K. In Recent Advances in Composite Materials: In Honor of S. A. Paipetis; Gdoutos, E. E.; Riga, Z.-M.; Paipetis, S. A., Eds.; Kluwer Academic Publisher, 2003; p 189.
26. Bazhenov, S. Polym Eng Sci 1995, 35, 813.
27. Berthelot, J.-M.; Fatmi, L. Eng Fract Mech 2004, 71, 1535.
28. Brito, Z.; Sànchez, G. Compos Struct 2000, 48, 79.
29. Einstein, A. Ann Phys 1906, 19, 289.
30. Smallwood, H. M. J Appl Phys 1944, 15, 758.
31. Guth, E. J Appl Phys 1945, 16, 20.
32. Kerner, E. H. Proc Phys Soc B 1956, 69, 808.
33. Lewis, T. B.; Nielsen, L. E. J Appl Polym Sci 1970, 14, 1449.
34. Mooney, M. J Colloid Sci 1951, 6, 162.
35. Brassell, G. W. J Mater Sci 1974, 9, 307.
36. Phillips, M. G. Compos Sci Technol 1992, 43, 95.
37. Miwa, M.; Takeno, A.; Hara, K.; Watanabe, A. Composites 1995, 26, 371.
38. Nielsen, L. E. J Appl Polym Sci 1966, 10, 97.
39. Nicolais, L.; Narkis, M. Polym Eng Sci 1971, 11, 194.
40. Gupta, A. K.; Purwar, S. N. J Appl Polym Sci 1984, 29, 3513.
41. Piggott, M. R.; Leidner, J. J Appl Polym Sci 1974, 18, 1619.
42. Turcsànyi, B.; Pukànsky, B.; Tûdos, F. J Mater Sci Lett 1988, 7, 160.
43. Bagwell, R. M.; Mc Manaman, J. M.; Wetherhold, R. C. Compos Sci Technol 2006, 66, 522.
44. Weidenfeller, B.; Höfer, M.; Schilling, F. R. Compos Part A Appl Sci Manuf 2004, 35, 423.
45. Mamunya, Y. P.; Davydenko, V. V.; Pissis, P.; Lebedev, E. V. Eur Polym Mater 2002, 38, 1887.